AAPT PHYSICS EDUCATION | AMERICAN JOURNAL of PHYSICS

Tethered particle motion with single DNA molecules

Dan Song, Briana Mousley, Stefano Gambino, Elsie Helou, Joseph Loparo, and Allen C. Price

Citation: American Journal of Physics **83**, 418 (2015); doi: 10.1119/1.4902187
View online: http://dx.doi.org/10.1119/1.4902187
View Table of Contents: http://scitation.aip.org/content/aapt/journal/ajp/83/5?ver=pdfcov
Published by the American Association of Physics Teachers

Tethered particle motion with single DNA molecules

Dan Song
Harvard Biophysics Program and Department of Biological Chemistry and Molecular Pharmacology, Harvard Medical School, Boston, Massachusetts 02115

Briana Mousley, Stefano Gambino, and Elsie Helou
Department of Chemistry and Physics, Emmanuel College, Boston, Massachusetts 02115

Joseph Loparo
Department of Biological Chemistry and Molecular Pharmacology, Harvard Medical School, Boston, Massachusetts 02115

Allen C. Price[a)]
Department of Chemistry and Physics, Emmanuel College, Boston, Massachusetts 02115

(Received 25 June 2014; accepted 10 November 2014)

A simple method for tethering microbeads using single molecules of DNA is explained. We describe how to use video microscopy and particle tracking to measure the trajectories of the microbeads' motion. The trajectories are analyzed and compared to different models of tethered particle motion. In addition, the data are used to measure the elasticity of the DNA (its spring constant), and the DNA persistence length.
[http://dx.doi.org/10.1119/1.4902187]

I. INTRODUCTION

Physical and quantitative methods are important tools in the study of biological mechanisms. Recognizing this, policy makers and educators alike have called for more rigorous training of future biologists in quantitative methods.[1] In addition, physics educators are actively working to train future scientists in biophysical techniques and concepts.[2] The techniques of single molecule biophysics (SMB) have contributed in great measure to our understanding of the biomolecular world. Although SMB is conceptually challenging, requiring background in physics and biology for a complete understanding, educators have made several advances in introducing these topics to undergraduates in the past several years. These contributions have included single molecule fluorescence,[3] optical trapping,[4] flow stretching of DNA,[5] fluctuation correlation spectroscopy,[6] and most recently, single ion channel recording.[7]

Many single molecule experiments require sophisticated and expensive equipment (e.g., fluorescence and optical trapping), leaving these techniques out of reach of many institutions. In previous work,[5] we have shown that DNA flow stretching can be used to make quantitative measurements of single molecules while requiring less sophisticated instrumentation than either optical trapping or single molecule fluorescence. Another promising technique is tethered particle motion (TPM), sometimes referred to as tethered Brownian motion. In the TPM technique, a DNA molecule is tethered to a fixed support at one end and to a microbead at the other (see Fig. 1). The microbead, visible using bright field microscopy, exhibits Brownian motion but is restrained by the tether. The technique has been used to measure DNA looping[8] and DNA mechanical properties,[9] as well as to screen for DNA-protein interactions.[10] Although simulations of this technique have been developed in an instructional context,[11] there has been little developed specifically for the undergraduate experimental laboratory.

In this paper, we report a TPM experiment designed for the undergraduate laboratory. In our experiment, students tether a single molecule of DNA and observe the Brownian motion of the tethered particle. By varying the length of the DNA, students explore the relation between tether length and the motion of the bead. In addition, quantitative analysis of the distribution of particle position allows students to directly determine mechanical properties of single DNA molecules.

The organization of this paper is as follows. In Sec. II, we describe the preparation and configuration of the components of the experiment, including the DNA, the sample cells, and the microscope and video camera. Section III describes the experimental procedures, which include DNA tethering, data collection, and preliminary data processing. In Sec. IV, we describe several ways that we have analyzed our data. These analyses vary in sophistication and are presented in order from the simplest to the most advanced. We conclude with suggestions for how the experiment can be extended.

II. EXPERIMENTAL DESIGN

In our tethered particle motion (TPM) experiment, a single double-stranded DNA (ds-DNA) molecule is immobilized at one end to a glass coverslip, while the other end of the polymer is attached to a microbead [Fig. 1(a)]. The motion of the bead is observed with video microscopy. In this section, we describe the design and creation of the DNAs, the construction of the sample cell, and the configuration of the microscope and video camera. Physicists may find the terminology used to describe the DNA preparation unfamiliar. However, the methods are standard and would be understood by anyone familiar with modern molecular biology. Interested readers are encouraged to consult their colleagues in biology or biochemistry departments. See also Refs. 12 and 13 for practical guides.

A. DNA

All DNAs must be labeled at one end with a biotin molecule for coupling to a microbead coated with streptavidin, a protein that binds biotin tightly. The other end of the DNA must be labeled with a digoxigenin molecule to tether to a glass cover slip coated with an antibody that binds the digoxigenin. We created three DNAs to study: (1) a 16.2-μm,

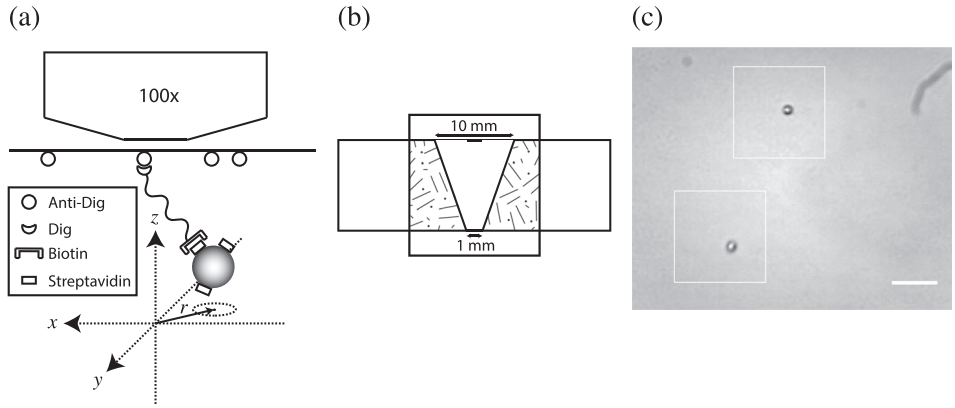

Fig. 1. Experimental design. (a) Schematic of experiment (not to scale). A single ds-DNA is tethered via a digoxigenin-antidigoxigenin antibody link to the surface and a biotin-streptavidin link to the bead (diameter = 1 μm). Projected x and y positions of the bead are measured with video microscopy. (b) Schematic of sample cell. The flow cell is assembled with a microscope slide, two pieces of double-sided tape, and a glass coverslip, and sealed with epoxy. (c) Typical image of tethered beads. The scale bar measures 6 μm.

48,502-base-pair (bp) DNA from bacteriophage λ (New England Biolabs, Inc.); (2) a 3.3 -μm, 10,000-bp segment of the bacterial genome isolated from *Bacillus subtilis* using a standard alkaline lysis procedure; and (3) a 0.33 -μm, 1,000-bp segment of the M13mp18 plasmid (New England Biolabs, Inc.). To end-label the λ DNA, biotin and digoxigenin labeled oligonucleotides (Integrated DNA Technologies, Inc.) complementary to each of the 12-nucleotide-long single-stranded overhangs on the linear λ ds-DNA are annealed and ligated sequentially. The end-labeled 10,000-bp and 1,000-bp ds-DNAs are constructed using a polymerase chain reaction (PCR) with custom designed primer pairs that are labeled with either biotin or digoxigenin (Integrated DNA Technologies, Inc.). The PCR products are purified using a Qiagen purification kit (Qiagen, Inc.). Detailed protocols are available in the electronic supplement to this article.[14] Streptavidin-coated paramagnetic microbeads of diameter 1 μm (Invitrogen, Dynabeads MyOne Streptavidin T1) are used as tethered particles.

B. Sample cell

The sample cell [Fig. 1(b)] is created by placing two pieces of double-sided tape at an angle across the center of a 3 in. × 1 in. microscope slide to form a trapezoidal channel with a 10-mm-wide entrance and a 1-mm-wide exit. The thickness of the tape determines the height of the channel. We found most commercial double-sided tapes as sold in office supply stores to make channels with heights of 50–80 μm. A 24 mm × 60 mm coverslip (No. 1.5) cut in half with a diamond scribe is placed on top of the tape and sealed firmly to expel air bubbles. The volume of the channel is estimated to be 10 μl. Sample loading and buffer exchange are done by pipetting the solution on the coverslip at the 10-mm-wide opening and then drawing the solution through to the 1-mm opening with a piece of Kimwipe. The trapezoidal shape of the channel maintains a low flow rate and reduces DNA shearing. After assembling the tethered complexes on the coverslip (described in Sec. III A), the edges of the flow cell and openings of the channel are sealed with epoxy to prevent evaporation.

C. Microscope and camera

An upright binocular microscope (Olympus CH30) with a 100× oil immersion objective is used to record the constrained Brownian motion of the tethered microbead under bright field illumination. A time-lapse video is acquired using an auto-exposure USB camera (Digital Microscope Imager, Celestron, Inc.) inserted into one eyepiece; video data are recorded using free video capture software.[15] The imaging resolution of our instrument is 0.12 μm/pixel as determined using a slide micrometer. See Fig. 1(c) for a typical still image from video data.

III. EXPERIMENTAL PROCEDURES

In this section, we start with a description of the tethering procedure and continue with how the video data are collected. We finish the section with a description of how the raw data in the form of video files are processed to create trajectories of bead positions.

A. Tethering DNA and microbeads

Before the cell is sealed with epoxy, DNA and microbeads must be introduced. To functionalize the sample cell for DNA tethering, 40 μl of 20 -μg/ml anti-digoxigenin antibody in phosphate buffered saline (137 mM NaCl, 2.7 mM KCl, 10 mM Na_2HPO_4, 1.8 mM KH_2PO_4, pH 7.4) is loaded into the sample cell and allowed to incubate for 30 min at room temperature. Note that in all incubation steps described here, it is helpful to leave a small drop of buffer at the entrance and exit to prevent evaporation in the channel. The channel is then washed with 40 μl of blocking buffer (20 mM Tris, 100 mM NaCl, 3 mg/ml BSA, pH 7.5) three times. Next, 40 μl of 20-pM DNA in blocking buffer (see Sec. II A, for preparation of DNA) is loaded and incubated for 30 min. The concentration of DNA can be adjusted to optimize binding efficiency. The numbers presented here should give one to two tethers per field of view when imaging under 100×. The channel is washed once more with 40 μl of blocking buffer before loading microbeads.

The microbeads are prepared at a concentration of 3.2 μg/ml in blocking buffer in order to get a ratio of beads to DNA of at least 10:1, to ensure no more than one DNA per bead. Magnetic beads make this step straightforward, as a magnetic separator can be used to pull down the beads for buffer exchange. Repeating the buffer wash a few times ensures complete buffer exchange. The bead suspension should be vortexed before loading in order to break up

aggregates. Forty microliters of the suspension is loaded into the sample cell and incubated for 30 min. One last wash step is performed before wiping off the edges of the channel and sealing with epoxy. Note that excessive washing after microbeads have been loaded can break DNA tethers. Prior to imaging, the sample cell is inverted so that the coverslip with tethered DNA-bead complexes is at the top of the channel.

B. Video data collection

Once the sample cell is mounted on the microscope, a tethered bead must be located. The procedure we use is to move progressively from the lowest-power objective (5×) to the highest (100×), locating the channel and beads after each change of objective. Tethered beads are identified by their motion and vertical location in the channel (attached to the upper surface). Once a tethered bead is centered in the field of view at highest magnification, data can be collected. The camera we use sets the exposure automatically, so we adjust the light level until the image of the bead appears such that it would be easy to track manually. (This criterion produces image quality sufficient for automatic tracking also; see Sec. III C.) The frame rate and data collection time should be set to collect a large number of independent samples of the bead position. Although the correlation time of the positional fluctuations depends on tether length (see Sec. V), a ten-minute video at 1 fps (producing 600 images) is sufficient for all the lengths of DNAs that we studied (from 0.3 μm to 16.2 μm).

C. Image processing

To process the data, the raw images must be converted into trajectories of (x, y) coordinates. First, we use the freely available image processing program IMAGEJ[16] to crop down the video to a size just large enough to cover the entire motion of an individual bead over time.

We investigated several methods for tracking. Manual tracking can be done using the Manual Tracking plugin[17] in IMAGEJ or the video tracking tools of LOGGERPRO.[18] In manual tracking, students click on the position of the bead and scroll through all images in the video. A 600-frame movie typically takes 15–20 min to process. We also developed custom tracking algorithms in MATLAB.[19] We used two methods: (1) calculating the bead's center-of-mass (COM) and (2) fitting a 2D Gaussian curve to the intensity data (see Appendix C). We compared these tracking methods and found that all yield similar results. All data reported here were tracked using the automatic COM method, as it was faster computationally. Figure 2(a) shows an example of tracking results for a single bead.

All analyses of processed data require measuring the position of the bead relative to the attachment point of the DNA. Sub-pixel resolution coordinates of the attachment point for each tethered particle can be determined by fitting a Gaussian to the histograms of the x and y coordinates of the bead. We additionally calculate the two-dimensional radial distance of the bead center from the attachment point according to the formula $r = \sqrt{x^2 + y^2}$ [see Fig. 1(a)]. We use the symbol r for the magnitude of the projected position vector of the bead in the two-dimensional tethering plane. We will reserve the symbol R for the magnitude of the three-dimensional position vector $R = \sqrt{x^2 + y^2 + z^2}$. An example histogram of the radial displacement of a single DNA tethered bead is shown in Fig. 2(b).

IV. INTERPRETATION OF RESULTS

The data collected in this experiment can be interpreted in a number of different ways, at a range of levels of sophistication. We review the different levels of our analysis that are appropriate at the undergraduate level in order from the simplest, appropriate for introductory courses, up to analyses that require more advanced mathematics and statistical mechanics. We close this section with a discussion of experimental artifacts and how to correct for them.

A. Dependence of TPM on tether length

The observation of tethered particle motion is in itself a worthwhile goal, as it will be the first (and possibly only) time students will directly see molecular-scale effects with their own eyes. Typically, an introduction to Brownian motion should precede a discussion of tethered particle motion. Then, before collecting and examining data, a student can be challenged to imagine what the effect of the

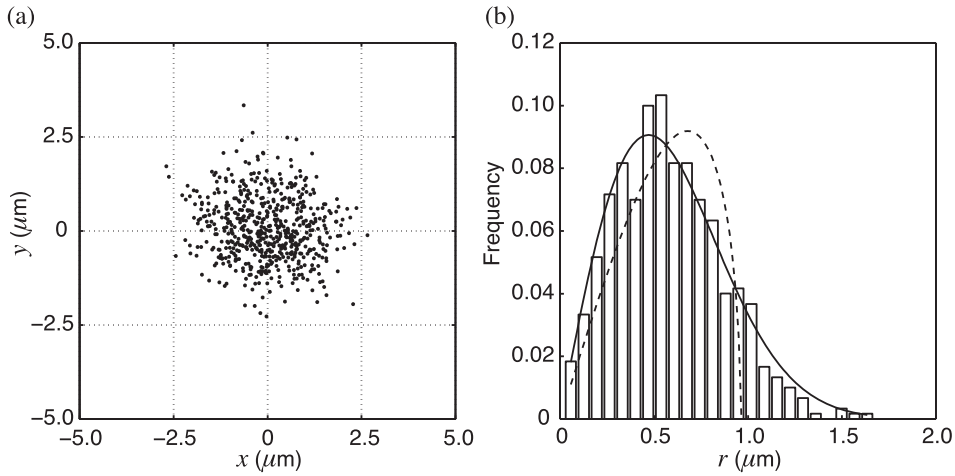

Fig. 2. Tracking of a DNA-tethered bead. (a) Scatter plot of a bead's center imaged for 600 s at 1 fps. (b) Histogram of the radial displacement of the bead center from the attachment point. The solid curve is fit to the tether-dominated model (fit yields a value of $\sigma = 0.91$ μm). The dashed curve is fit to the bead-dominated model discussed in text.

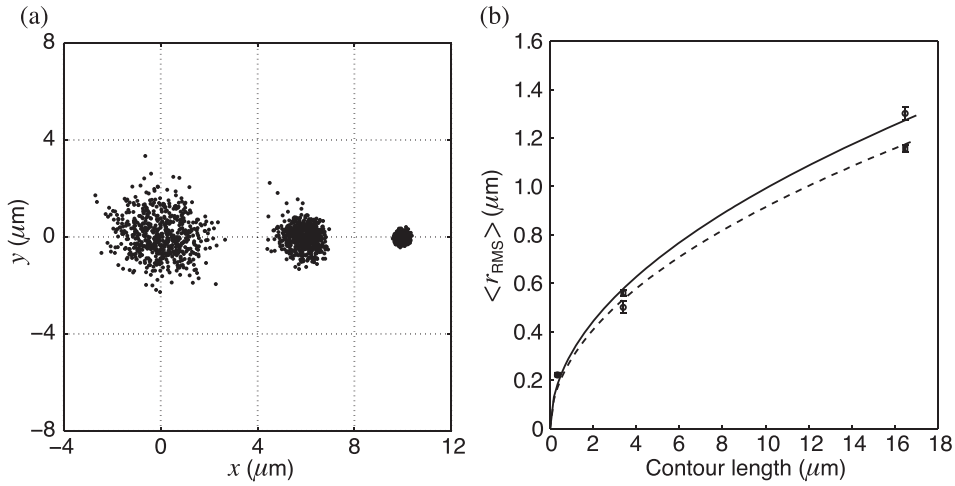

Fig. 3. Variation of TPM with contour length of DNA. (a) Scatter plots of x and y coordinates of beads for 16.2 μm (left), 3.3 μm (middle), and 0.3 μm (right) DNA. (b) The RMS displacement averaged over beads is proportional to the square root of the DNA contour length. The upper fit is to uncorrected data and yields a Kuhn length of 150 ± 60 nm. The lower fit is to data corrected for drift and yields a Kuhn Length of 130 ± 40 nm.

tether will be on the motion. One way to treat the data at an introductory level is to address the question of how the tether length (in this case, the length of the DNA when fully stretched, also known as the contour length) affects the motion of the bead. The question is important in applications of TPM to DNA looping, as looping changes the effective tether length[20] but not the contour length. As the tether length and the contour length are the same in the absence of looping, we will refer to the contour length in this section.

We had students collect data using DNAs of three different lengths: 0.33 μm, 3.3 μm, and 16.2 μm (see Sec. II A). Figure 3(a) shows scatter plots of bead positions for typical data. In order to quantify the width of the distribution of the positions, we use the two-dimensional projected radial coordinate r of the bead center relative to the tethering point. We determine the root-mean-squared radial coordinate, $r_{\mathrm{RMS}} = \sqrt{\langle r^2 \rangle}$, by averaging over all observed bead positions for a single DNA. Figure 3(b) shows the average of r_{RMS} for several measurements plotted versus the contour length of the DNA. One can clearly see that the width of the distribution increases monotonically with contour length.

An unconfined, long flexible polymer is known to obey a simple scaling relation. To understand this relation, consider the three-dimensional end-to-end distance of the polymer, $R = \sqrt{x^2 + y^2 + z^2}$ (see Fig. 4 for an illustration). If we now define the RMS end-to-end distance (averaged over all conformations of the DNA) as $R_{\mathrm{RMS}} = \sqrt{\langle x^2 \rangle + \langle y^2 \rangle + \langle z^2 \rangle}$, then the scaling relation says that $R_{\mathrm{RMS}} = \sqrt{bL}$, where L is the contour length of the polymer and the constant b is known as the Kuhn length.[21] Although our polymer is confined to a half-space, we can make the crude approximation that the mean-squared displacements in the unconfined directions ($\langle x^2 \rangle$ and $\langle y^2 \rangle$) have the same values as for the fully unconfined (untethered) polymer. Using this approximation, and the fact that for the fully unconfined polymer $\langle x^2 \rangle = \langle y^2 \rangle = \langle z^2 \rangle$, we find that $\langle r^2 \rangle = \frac{2}{3} bL$, where $r^2 = x^2 + y^2$. Using this relation, the fit shown in Fig. 3(b) yields a Kuhn length of 150 ± 60 nm, which is only slightly larger than the accepted value for ds-DNA of around 100 nm.[22] Our determination of this parameter is crude, as it does not consider the effects of nonzero bead size or deal correctly with the volume-exclusion effects of the surface.[23]

B. Comparing different models of TPM

The distributions of the particle position [Fig. 2(b)] show a specific dependence on distance from the tether point. To begin to understand this particular form, we need to think about models of the system. Using and evaluating models is an important scientific ability that warrants explicit inclusion in coursework.[24] We investigated if students could use the data provided in this experiment in an exercise in discrimination between competing models of tethered particle motion. We devised two models that can be used to derive predictions for the form of the distribution of particle position. We found the quality of the data to be sufficient to discriminate between these two models.

In the first model (the "bead-dominated" model), the effect of the tether is to restrain the bead from moving more than a distance of $d = L + a$, where L is the contour length of the DNA and a is the bead radius. When the center of the bead is less than d away from the tether point, the motion of the bead is free Brownian motion. In this simple model, we ignore the effect of any force from the DNA on the bead unless the DNA is completely extended. We also postpone consideration of any other effects of the nonzero size of the bead (such as steric interactions) until Sec. IV E. The

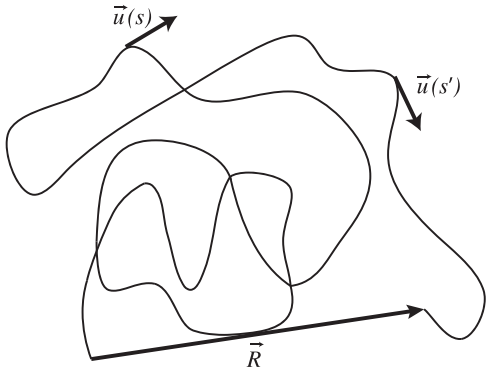

Fig. 4. Conformation of the DNA. The DNA is tethered to a fixed point at bottom left. The end-to-end vector $\vec{R}$ goes from the tether point to the free end. Unit tangent vectors $\vec{u}$ are shown at two points, s and s', as measured from the tether point.

immediate consequence of this physical picture is that the bead can be found with equal probability anywhere under a hemisphere of radius d. In Appendix A, we derive from this model the probability density for the radial distance r. The result is

$$P_r(r) = \frac{3r}{d^2}\sqrt{1-\left(\frac{r}{d}\right)^2}. \tag{1}$$

Equation (1) is valid only for $r < d$; the probability density is zero for $r > d$.

In the second model (the "tether-dominated" model), we assume that the position of the bead is determined by the random conformation of the DNA. In this model, the bead simply reports the position of the end of the random chain. The distribution of the bead positions is then simply the same as the distribution of the end of a long tethered flexible polymer. Here also, discussion of the effects of bead size will be left to Sec. IV E. It is a well-known result from the statistical mechanics of polymers that the end-to-end vector of a long flexible polymer obeys a Gaussian distribution.[21] However, deriving this result is typically out of reach of most undergraduate students. The result can be understood as an application of the central limit theorem: the end position of the polymer is the result of adding up a large number of segmental vectors that are each statistically independent. An alternative motivation relies on the fact that the normal distribution, as the Gaussian distribution is known in statistics, is a common mathematical model for random variables distributed about a mean value. Assuming a Gaussian distribution, the probability density for finding the particle at a distance r from the tether point (as measured in the tethering plane) is

$$P_r(r) = \frac{r}{\sigma^2}\exp\left(-\frac{r^2}{2\sigma^2}\right), \tag{2}$$

where σ is a numerical parameter of the model and quantifies the width of the distribution.

The method employed to test these models is to fit Eqs. (1) and (2) to radial histograms of the bead position and examine quality of fit. We included an extra multiplicative factor to account for unnormalized data. An example of the fits is shown in Fig. 2(b), which shows the fits of the two model predictions to data from λ DNA (16.2-μm long). It is clear that the tether-dominated model fits the data much better. Moreover, the fit of the bead-dominated model yields an incorrect contour length (about 1 μm). However, one can see that knowledge of the actual contour length is not necessary to reject the bead-dominated model. The predicted distribution for that model falls off to zero far too rapidly (with negative curvature) and cannot explain the tail of the data. Students can use this result to reason that the statistical mechanics of the DNA exerts a significant influence on the behavior of the tethered particle.

C. Determining the persistence length of DNA

The persistence length is an important concept from the statistical mechanics of polymers. The derivation of the relation between the persistence length and the width of the distributions we measure in this experiment offers an opportunity to apply the concepts of correlation functions and ensemble averages in an important yet likely new context for the student. We used our data to attempt to determine the persistence length for our DNAs.

The persistence length can be thought of as the distance over which the DNA maintains its direction. It is the correlation length (as measured along the DNA) of the directional fluctuations of the DNA segments. DNA molecules much longer than this length are coiled randomly. The mathematical definition of the persistence length is given in Appendix B, as is a derivation of the formula relating the mean-squared end-to-end distance of a polymer $\langle R^2\rangle$ to the persistence length P. Here, we simply quote the result: $\langle R^2\rangle = 2PL$, for $L \gg P$.

The preceding result is derived for a polymer that is not confined to a half space ($z > 0$). If we assume that the presence of the confining plane does not affect the fluctuations in the directions parallel to the plane, then we expect that $\langle r^2\rangle = \frac{2}{3}\langle R^2\rangle$, where R^2 is the mean-squared end-to-end distance for an *unconfined* polymer. Solving for the persistence length in terms of the measured quantity then yields

$$P = \frac{3}{4}\frac{\langle r^2\rangle}{L}. \tag{3}$$

We calculated $\langle r^2\rangle$ for our data for λ DNA and used Eq. (3) to determine the persistence length. Figure 5(a) shows a histogram of results for several experiments. The mean and standard deviation of these determinations is 84 ± 26 nm. Although a recent experiment using TPM with shorter DNAs and smaller beads has given results from 10 to 80 nm,[9] most published values for the persistence length of DNA measured using other techniques are close to 50 nm.[22] Our measurement is larger than this, a result that can be ascribed to lack of correction for drift and nonzero bead size (see Sec. IV E).

D. Measuring the spring constant of DNA

In this section, we apply statistical mechanics to TPM at a level appropriate for an upper-division undergraduate course. We model the effect of the DNA on the bead as a linear spring and derive the complete probability distribution for the position of the bead. The value of the spring constant of the DNA can then be calculated from the experimentally determined width. We also compare our results to the nonlinear "worm-like-chain" interpolation formula, which is routinely used to model the force-extension behavior of DNA.

We assume that the only effect the DNA has on the bead position is to exert a restoring force that increases linearly with the distance of the bead from the attachment point and is directed towards the attachment point. Discussion of bead size effects will be reserved for Sec. IV E. The surface is assumed to affect the system only by limiting z to positive values (see Fig. 1(a) for the coordinate system). Assuming a simple force law $F = KR$, where R is the three-dimensional distance from the tether point and K is the spring constant of the DNA, the potential energy is $U = \frac{1}{2}KR^2$. The configurational partition function for this system is then

$$\begin{aligned} Z &= \int_{z>0} dV\, e^{-\beta U} \\ &= \int_{-\infty}^{\infty} dx \int_{-\infty}^{\infty} dy \int_{0}^{\infty} dz\, \exp\left[-\frac{K\left(x^2+y^2+z^2\right)}{2k_BT}\right] \\ &= \frac{1}{2}\left(\frac{2\pi k_BT}{K}\right)^{3/2}, \end{aligned} \tag{4}$$

where k_B is Boltzmann's constant and T is the temperature.

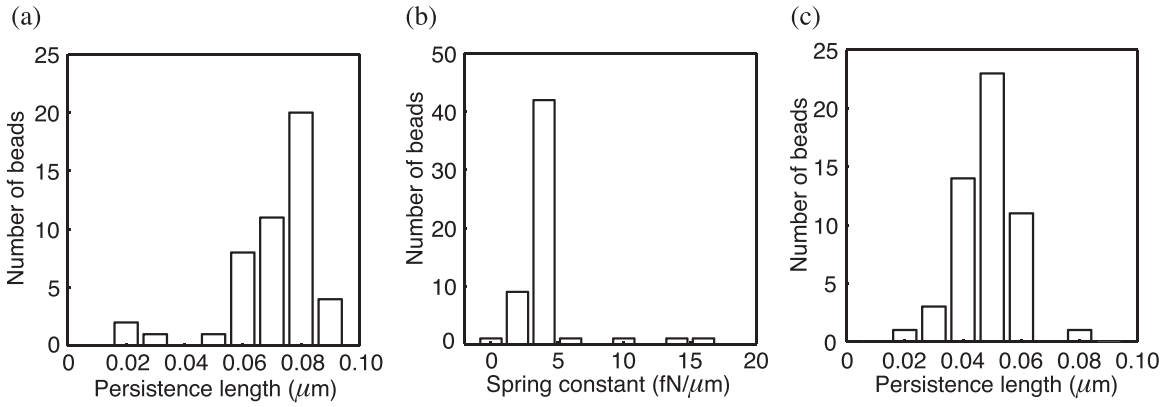

Fig. 5. Physical properties of DNA determined using TPM. (a) Histogram of persistence lengths as measured for 16.2-μm DNA (uncorrected data). Persistence lengths of individual DNAs were determined as discussed in text using $P = \frac{3}{4}\langle r^2\rangle/L$. The mean and standard deviation of the values shown are 84 ± 26 nm. (b) Histogram of spring constants as measured for 16.2-μm DNA. Spring constants of individual DNAs were determined from widths of positional distributions using $K = k_BT/\sigma^2$, as described in text. The mean and standard deviation of the values shown are 5.0 ± 2.4 fN/μm. (c) Histogram of persistence lengths as measured for 16.2-μm DNA using data corrected for drift and nonzero bead size. The mean and standard deviation of the values shown are 54 ± 12 nm.

The probability density for the bead position coordinates in the plane perpendicular to the optic axis [here assumed to be the z-direction, see Fig. 1(a)] can be determined from the above expression by not doing the integrals in x and y, and then normalizing the result by dividing by the partition function. The result is the two-dimensional Gaussian distribution

$$P_\perp(x,y) = \frac{K}{2\pi k_BT}\exp\left[-\frac{K(x^2+y^2)}{2k_BT}\right]. \tag{5}$$

By integrating this expression over the azimuthal angle and switching variables to $r = \sqrt{x^2+y^2}$, we get the probability density for the radial coordinate

$$P_r(r) = \frac{Kr}{k_BT}\exp\left(-\frac{Kr^2}{2k_BT}\right). \tag{6}$$

Note that this formula is of the same form as in Eq. (2) but with an explicit value of $\sigma^2 = k_BT/K$. Figure 2(b) shows a histogram of the radial coordinate of the bead for data from λ DNA. Assuming a temperature of 297 K, the fit yields a value for the spring constant of the DNA equal to 5 fN/μm. Figure 5(b) shows a histogram of measured spring constants for several DNAs. The mean and standard deviation of these measurements is 5 ± 2 fN/μm.

Although we modeled the DNA with a linear restoring force, the full nonlinear force response of λ DNA has been accurately measured[22] and compares well to a theoretical prediction from the worm-like-chain model,[25] where the DNA is treated as a flexible polymer with a finite bending rigidity. The derivation of the full nonlinear force law is beyond the scope of this paper, but the following interpolation formula is useful:[25]

$$F = \frac{k_BT}{P}\left[\frac{1}{4(1-R/L)^2} - \frac{1}{4} + \frac{R}{L}\right]. \tag{7}$$

The P in this formula is the persistence length of the DNA defined in Appendix B, and L is the contour length. The limit of this equation for small extensions yields a linear force law

$$F \approx \frac{3k_BT}{2PL}R. \tag{8}$$

Using the accepted value for the persistence length (50 nm), we calculate a theoretical spring constant of 7.7 fN/μm for λ DNA. The difference between our measurement and the accepted value can be attributed to drift and nonzero bead size effects, which will be treated in Sec. IV E.

E. Experimental artifacts

In single-molecule experiments, correcting for artifacts can be a crucial step in the analysis. In our experiments, there are four effects that can alter the results significantly. In all four cases, either the effects can be corrected or the resulting outliers can be rejected. These effects are drift, non-specific interactions, multiple tethering, and nonzero bead size.

1. Drift

Trajectories of the x and y displacements of the bead center from the attachment point reveal a slow variation due most likely to stage or other mechanical drift. A drift correction can be performed by time-averaging the data with a time window of 100 s (see Fig. 6). The smoothed data are then subtracted from the raw data to yield the drift-corrected data [see Fig. 6(a)]. Figures 6(b) and 6(c) show how drift biases a tethered bead's symmetric motion around the attachment point.

2. Non-specific interactions and multiple tethering

Non-specific interactions with the surface or multiple DNAs tethering a bead can alter the bead motion in complicated ways. (The term "non-specific interactions" refers to any unintended interactions between the bead and the surface that can affect the bead's motion.) Some typical effects can be reduced motion of the bead and asymmetric positional distributions. To discard these outliers that exhibit minimal Brownian motion, a threshold is determined after plotting a histogram of the radial displacement. Visual inspection for symmetric distributions (after drift correction) can eliminate

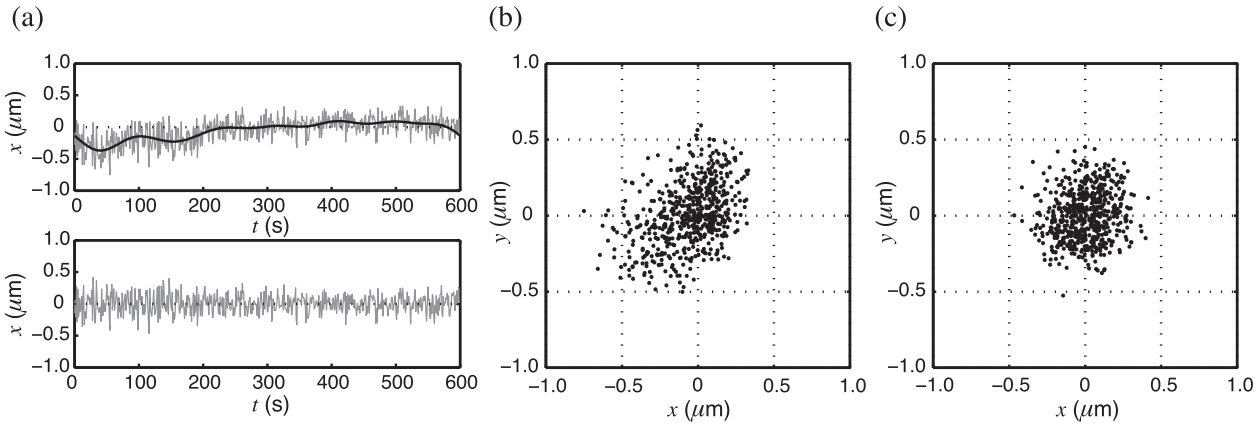

Fig. 6. Effects of drift. (a) Trajectory of x-displacements of the bead center for 0.3-μm DNA before (top) and after (bottom) correcting for drift. The solid curve is data smoothed with a low-pass filter (cutoff frequency 0.01 Hz). To the right are scatter plots of the bead position before (b) and after (c) correction.

some multiple tethering. Symmetric distributions of the tethers can also be tested by calculating the covariance matrix of the x and y displacements.[26] A threshold on the ratio of the eigen values of the covariance matrix can make such selection automatic (note that this is the ratio of the major and minor axes of the distribution modeled as an ellipsoid).

3. Nonzero bead size

The nonzero size of the bead is properly considered not as a source of error, but as a property of the system that must be correctly taken into account when interpreting the data. A theoretical treatment of nonzero bead size in TPM, accounting for the steric interactions ("volume exclusion") between the surface and the bead, shows that the mean-squared displacement parallel to the tethering plane satisfies[23]

$$\frac{\langle r^2 \rangle}{LP/3} = 2 + \frac{4N_a}{\sqrt{\pi}\,\mathrm{erf}(N_a)}. \tag{9}$$

Here, "erf" is the error function and N_a is the "excursion number," which is defined as $N_a = a/\sqrt{LP/3}$, where a is the radius of the bead. Note that the excursion number is proportional to the ratio of the bead size to the RMS end-to-end distance of the DNA in the small-bead limit. If $N_a \ll 1$, then the particle does not alter the observed behavior significantly from the "free end" limit. In our case, with $a = 0.5\mu$m, $L = 16.2\mu$m, and $P = 50$ nm, the excursion number is about 1, and we can expect the nonzero bead size to influence our measurements significantly.

To correct for the nonzero bead size in the persistence length measurement, one can use the measured variance in bead position and solve Eq. (9) numerically for P. The results of applying this correction to the data shown in Fig. 5(a) are shown in the accompanying panel, Fig. 5(c). The trajectories that went into this data were corrected for drift and filtered as described above. The mean and standard deviation of these corrected measurements are 54 ± 12 nm, in agreement with prior results.[22]

V. CONCLUSIONS

In this paper, we have described a single-molecule biophysics experiment appropriate for the undergraduate. Versions of the experiment can be performed with students from introductory or upper-division courses. Students are exposed to basic concepts in single-molecule biophysics, as well as theoretical concepts in polymer mechanics.

Our experiment can be extended a number of ways. By collecting at a higher frame rate and calculating the autocorrelation of the bead position, students can determine the correlation time of the dynamic fluctuations of the bead. The decay time of the autocorrelation function can be related to the diffusion constant of the bead and the tether length.[27] Protein-DNA interactions can be observed by introducing proteins that form loops in DNA.[28] Another possibility is to look at the effect of reversible or irreversible chemical modifications of the DNA. Intercalating agents, such as some fluorescent dyes, insert between the bases in DNA and increase the overall contour length.[29] The cancer drug cisplatin reacts irreversibly with DNA, causing kinks in the DNA structure that shorten its persistence length.[30] All of these phenomena have been studied using TPM.

One barrier to implementation of single-molecule biophysics in physics curricula is the unfamiliarity that many physics instructors have with the techniques of molecular biology (the tool kit of techniques for creating DNA constructs). The techniques used in this work are easy to learn and require little in the way of instrumentation. The authors hope that this work will contribute to lowering the barrier to the widespread introduction of biophysical experiments on DNA in the undergraduate laboratory.

ACKNOWLEDGMENTS

The authors would like to acknowledge Wendy Gordon for supplying the 1-kb DNA and Thomas Graham for supplying the 10-kb DNA. The authors also thank Maximilian Benz for his help in collecting some of the data reported in this work. This work was made possible by the support of Emmanuel College and the National Science Foundation. J.L. was supported by NSF CAREER Award MCB-1148818; A.C.P. was supported by NSF RUI Award PHY-1205814.

APPENDIX A: THE RADIAL DISTRIBUTION FOR THE BEAD-DOMINATED MODEL

In this Appendix, we derive the distribution for the radial coordinate of the bead position as predicted by the model discussed in Sec. IV B. We assume that the only effect of the

tether is to restrain the bead from moving more than a distance d from the tether point. Steric interactions between tether and bead are ignored. The only effect of the surface, then, is to limit the values of the z-coordinate to $z > 0$. Under these assumptions, the bead can be found with equal probability anywhere within a hemisphere of radius d. Since the volume of the allowed region is $2\pi d^3/3$, the probability density for the position of the particle is

$$P(\vec{R}) = \frac{3}{2\pi d^3} \tag{A1}$$

for $R < d$ and $P(\vec{R}) = 0$ otherwise.

Because we observe only the coordinates of the bead perpendicular to the optic axis, we must integrate this expression along the coordinate perpendicular to the tethering plane. Since the expression is constant inside the hemispherical region and zero outside, we simply get the height of the sphere

$$P_\perp(x,y) \equiv \int_0^{\sqrt{d^2-x^2-y^2}} \frac{3}{2\pi d^3}\, dz = \frac{3}{2\pi d^2}\sqrt{1-\left(\frac{x}{d}\right)^2-\left(\frac{y}{d}\right)^2}. \tag{A2}$$

The final transformation necessary to make our results applicable to our data analysis is to determine the probability density of the radial coordinate. We multiply the expression in Eq. (A2) by the expression for a small area in the plane in terms of polar coordinates ($dA = rd\theta dr$), integrate over θ, and divide by dr to get

$$P_r(r) = \frac{3r}{d^2}\sqrt{1-\left(\frac{r}{d}\right)^2}. \tag{A3}$$

Note that this equation is valid only for $r < d$. For $r > d$, the probability density is zero. This expression shows that the radial distribution should be zero at $r = 0$ and for $r \geq d$, which makes sense. One feature of this result that is seen clearly in Fig. 2(b) is that the *curvature* of the distribution is always negative.

APPENDIX B: DEPENDENCE OF WIDTH OF DISTRIBUTION ON PERSISTENCE LENGTH

In this Appendix, we derive the relation between the variance in the end-to-end distance of a long flexible polymer and its persistence length. We will first define the persistence length in terms of fundamental properties of the polymer, and then derive an expression for the end-to-end vector of the polymer. Evaluating the mean of the squared integral will give us the relation we seek.

First, we define the unit tangent vector $\vec{u}(s)$ as a function of the position along the DNA contour (see Fig. 4). The position s is measured as the distance along the DNA (as an ant would crawl) starting from the tether point, and the direction of the vector is towards the free end. Next we define the "directional correlation function" as the ensemble average of the inner product between two unit tangent vectors taken at distinct points along the polymer

$$C(s,s') \equiv \langle \vec{u}(s)\cdot\vec{u}(s')\rangle. \tag{B1}$$

The brackets indicate an average over all the possible conformations of the molecule. If the points s and s' are far from the ends of the polymer, we can expect this quantity to depend only on the distance $|s-s'|$ between the points.

The detailed conformations the polymer can assume depend on the microscopic properties of the molecule (whether it has some rigidity, rotatable bonds, and so on). However, for a broad class of polymers the directional correlation function takes an exponential form[21]

$$\langle \vec{u}(s)\cdot\vec{u}(s')\rangle = \mathrm{e}^{-|s-s'|/P}. \tag{B2}$$

The quantity P is the "persistence length" and can be thought of as the distance (as the ant crawls) over which the DNA maintains its direction. On length scales longer than this it looks floppy and is, in general, quite coiled.

We now consider the "end-to-end" displacement (as the crow flies), which is shown in Fig. 4, labeled $\vec{R}$. The magnitude of $\vec{R}$ is important experimentally because it represents the "size" of the coiled-up DNA. The end-to-end vector can be calculated from the unit tangent vector using the relation

$$\vec{R} = \int_0^L \vec{u}(s)\, ds, \tag{B3}$$

where the integral runs from the tether point to the free end. We can calculate the average of the square of the end-to-end distance simply by taking the dot product of this expression with itself and averaging over the ensemble to arrive at

$$\langle R^2\rangle = \int_0^L ds \int_0^L ds' \langle \vec{u}(s)\cdot\vec{u}(s')\rangle = \int_0^L ds \int_0^L ds' e^{-|s-s'|/P}, \tag{B4}$$

where we have use Eq. (B2) for the integrand. This integral can be evaluated to give

$$\langle R^2\rangle = 2PL\left[1-\frac{P}{L}\left(1-e^{-L/P}\right)\right]. \tag{B5}$$

For the DNAs in our experiments, $L \gg P$ (for the longest DNA $L/P \approx 320$ and for the shortest $L/P \approx 7$); the relation then simplifies to $\langle R^2\rangle \approx 2PL$.

APPENDIX C: AUTOMATIC TRACKING ALGORITHM

To distinguish a bead of interest from the background, an image mask is created by applying an intensity and an area threshold on the original gray-scale image. Specifically, a background intensity is calculated as the median of the total intensities. After subtracting the background, the image is squared to enhance edge detection of the bead. A binary image mask is created by first selecting pixels with intensities that are above an empirically determined threshold. Then the intensities of selected pixels are set to 1 and those that remain are set to 0. Holes in the mask as a result of nonhomogeneity at the center of a bead are filled with a MATLAB built-in function called `imfill`. Speckles of noise with high intensities sometimes are mistakenly picked up during intensity thresholding. Thus, objects with areas that are below a threshold are considered to be background and their

intensities are set to 0. Finally, the binary image mask is multiplied to the original gray-scale image for further determination of a bead's center.

For a gray-scale image with a dimension of $m \times n$ pixels, the center-of-mass coordinates $(x_{\mathrm{COM}}, y_{\mathrm{COM}})$ are calculated as

$$x_{\mathrm{COM}} = \frac{\sum_{j=1}^{n} \mathrm{ProjRow}_j \cdot j}{\sum_{i=1}^{m}\sum_{j=1}^{n} I_{ij}}, \tag{C1}$$

$$y_{\mathrm{COM}} = \frac{\sum_{i=1}^{m} \mathrm{ProjCol}_i \cdot i}{\sum_{i=1}^{m}\sum_{j=1}^{n} I_{ij}}, \tag{C2}$$

where I_{ij} is the intensity value at the ith row and jth column of the image, ProjRow is the projection of the image into a row defined as $\sum_{i=1}^{m} I_{ij}$, and ProjCol is the projection of the image into a column defined as $\sum_{j=1}^{n} I_{ij}$.

Alternatively, the projection of an image in each dimension can be fitted with a Gaussian function defined as

$$\mathrm{ProjRow} = A \exp\left[\frac{-(x - x_0)^2}{2\sigma^2}\right] + B, \tag{C3}$$

where A and B are constants, x_0 is the mean, and σ is the standard deviation.

Coordinates of the center of a bead are the fitted mean values (x_0, y_0).

[a]Electronic mail: priceal@emmanuel.edu

[1]National Research Council Committee on Undergraduate Biology Education to Prepare Research Scientists for the 21st Century, *Bio2010: Transforming Undergraduate Education for Future Research Biologists* (The National Academies Press, Washington, DC, 2003), pp. 60–74.
[2]M. Sabella and M. Lang, "Research and education at the crossroads of biology and physics," Am. J. Phys. **82**(5), 365–367 (2014).
[3]J. Zimmermann, A. van Dorp, and A. Renn, "Fluorescence microscopy of single molecules," J. Chem. Ed. **81**(4), 553–557 (2004).
[4]D. C. Appleyard, K. Y. Vandermeulen, H. Lee, and M. J. Lang, "Optical trapping for undergraduates," Am. J. Phys. **75**(1), 5–14 (2007).
[5]K. Burke, B. Grafe, K. Williams, N. Tanner, A. M. van Oijen, J. Loparo, and A. C. Price, "A single molecule DNA flow stretching microscope for undergraduates," Am. J. Phys. **79**, 1112–1120 (2011).
[6]R. Rieger, C. Röcker, and G. U. Nienhaus. "Fluctuation correlation spectroscopy for the advanced physics laboratory," Am. J. Phys. **73**(12), 1129–1134 (2005).
[7]Y. Klapper, K. Nienhaus, C. Röcker, and G. U. Nienhaus, "Lipid membranes and single ion channel recording for the advanced physics laboratory," Am. J. Phys. **82**(5), 502–509 (2014).
[8]F. Vanzi, C. Broggio, L. Sacconi, and F. S. Pavone, "Lac repressor hinge flexibility and DNA looping: single molecule kinetics by tethered particle motion," Nucleic Acids Res. **34**(12), 3409–3420 (2006).
[9]S. Brinkers, H. R. Dietrich, F. H. de Groote, I. T. Young, and B. Rieger, "The persistence length of double stranded DNA determined using dark field tethered particle motion," J. Chem. Phys. **130**(21), 215105 (2009).
[10]T. Plenat, C. Tardin, P. Rousseau, and L. Salome, "High-throughput single-molecule analysis of DNA-protein interactions by tethered particle motion," Nucleic Acids Res. **40**(12), e89.1–e89.8 (2012).
[11]J. F. Beausang, C. Zurla, L. Finzi, L. Sullivan, and P. C. Nelson, "Elementary simulation of tethered Brownian motion," Am. J. Phys. **75**(6), 520–523 (2007).
[12]D. D. Moore and D. Dowhan, "Preparation and analysis of DNA," in *Current Protocols in Molecular Biology*, edited by F. M. Ausubel (Wiley, New York, 2010).
[13]K. Struhl, "Enzymatic manipulation of DNA and RNA," in *Current Protocols in Molecular Biology*, edited by F. M. Ausubel (Wiley, New York, 2010).
[14]See EPAPS Document No. http://dx.doi.org/10.1119/1.4902187 for experimental protocols or <http://allenprice.blogs.emmanuel.edu/teaching/>.
[15]SKYSTUDIOPRO software, <http://www.skystudiopro.com/>.
[16]National Institutes of Health, IMAGEJ software, <http://imagej.nih.gov/ij/>.
[17]The manual tracking plugin for IMAGEJ can be downloaded from <http://rsbweb.nih.gov/ij/plugins/track/track.html>.
[18]Vernier Software & Technology, LOGGERPRO software, <http://www.vernier.com/products/software/>.
[19]The Mathworks, Inc., MATLAB software, <http://www.mathworks.com/products/matlab/>.
[20]P. C. Nelson, C. Zurla, D. Brogioli, J. F. Beausang, L. Finzi, and D. Dunlap, "Tethered particle motion as a diagnostic of DNA tether length," J. Phys. Chem. B **110**(34), 17260–17267 (2006).
[21]A. R. Khokhlov and A. Y. Grosberg, *Statistical Physics of Macromolecules* (AIP Press, New York, 1994), pp. 14–20.
[22]C. Bustamante, J. F. Marko, E. D. Siggia, and S. Smith, "Entropic elasticity of lambda phage DNA," Science **265**, 1599–1600 (1994).
[23]D. E. Segall, P. C. Nelson, and R. Phillips, "Volume-exclusion effects in tethered-particle experiments: bead size matters," Phys. Rev. Lett. **96**(8), 088306 (2006).
[24]E. Etkina, A. Warren, and M. Gentile, "The role of models in physics education," Phys. Teach. **44**(34), 34–39 (2006).
[25]J. F. Marko and E. D. Siggia, "Stretching DNA," Macromolecules **28**, 8759–8770 (1995).
[26]B. Lui, L. Han, S. Blumberg, J. F. Beausang, P. C. Nelson, and R. Phillips, "Calibration of tethered particle motion experiments," in *Mathematics of DNA Structure, Function and Interactions*, edited by C. J. Benham, S. Harvey, W. K. Olson, D. W. Sumners, and D. Swigon (Springer, New York, 2009), pp. 123–138.
[27]K. B. Towles, J. F. Beausang, H. G. Garcia, R. Phillips, and P. C. Nelson, "First-principles calculation of DNA looping in tethered particle experiments," Phys. Biol. **6**(2), 025001 (2009).
[28]C. Zurla, C. Manzo, D. Dunlap, D. E. Lewis, S. Adhya, and L. Finzi, "Direct demonstration and quantification of long-range DNA looping by the lambda bacteriophage repressor," Nucleic Acids Res. **37**(9), 2789–2795 (2009).
[29]K. Gunther, M. Mertig, and R. Seidel, "Mechanical and structural properties of YOYO-1 complexed DNA," Nucleic Acids Res. **38**(19), 6526–6532 (2010).
[30]Z.-Q. Sun, W. Li, P. Xie, S.-X. Dou, W.-C. Wang, and P.-Y. Wang, "Elastic response and length change of single DNA molecules induced by a combination of cisplatin and transplatin," Phys. Rev. E **85**, 021918 (2012).